***Journal of Education and Science (ISSN 1812-125X)***

www.edusj.uomosul.edu.iq

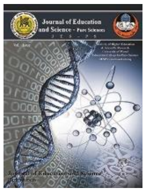

# Indirect Estimation of Free Prostatic Specific Antigen (FPSA) on Glassy Carbon Electrode Through its Interaction with Manganese Acetate Using Differential Pulse Voltammetric Technique

**M. Q. Hasan(1)*, A. Th. Al-Taee(2), M. A. Al-Imam(3)**

(1,2) Department of Chemistry, College of Science, University of Mosul, Mosul, Iraq
(3) Department of Chemistry, College of Education for Pure Science, University of Mosul, Mosul, Iraq

**Article information**

***Article history:***
**Received: April 21, 2025**
**Revised: June 13, 2025**
**Accepted: June 17, 2025**
**Available online: July 01, 2025**

***Keywords*:**
FPSA
Glassy Carbon
Indirect Determination

***Correspondence:***
**Mohammed Q. Hasan**
moh.hasan@uomosul.edu.iq

**Abstract**

Indirect electrochemical properties characteristics of free prostate-specific antigen (FPSA) were investigated using the differential pulse voltammetric (DPV) technique, employing a three-electrode system. This setup included a 2 mm diameter glassy carbon electrode as the working electrode, a 2 mm diameter platinum wire serving as the auxiliary electrode, and a silver/silver chloride saturated potassium chloride electrode as the reference electrode. (Ag/AgCl sat KCl). The method is based on observing the decrease in the manganese acetate reduction peak current which is due to its interaction with FPSA. Acetate buffer solution (pH4) was used, the potential scanned between -1.0 V to 0.5V and the optimum conditions were tested. A calibration curve for free prostate-specific antigen (FPSA) was established based on a series of sequential additions of the analyte. The response to FPSA additions was linear within the studied concentration range (5.4980 - 13.6633) x$10^{-7}$ M, with a correlation coefficient of 0.9581 and calibration equation y = 0.0073x + 0.6451. The binding constant (k), as well as the values of $\Delta G$, $\Delta H$, and $\Delta S$ were calculated to assess the thermodynamic characteristics of the $Mn^{+2}$- FPSA binding.

DOI: 10.33899/edusj.2025.159381.1557, ©Authors, 2025, College of Education for Pure Science, University of Mosul.

## 1. Introduction

Prostate cancer (PCa) is among the most serious health threats facing men over the age of 50, primarily due to its asymptomatic nature in the early stages. As a result, extensive research has focused on identifying reliable biomarkers for PCa and developing technologies for their application in clinical settings. One of the earliest biomarkers utilized for PCa diagnosis and staging was prostatic acid phosphatase (PAP). However, the challenge of precisely measuring the prostate-specific production of this isoenzyme led researchers to search for more dependable diagnostic alternatives over the years. A follow-up study demonstrated that PSA (prostate-specific antigen) could be detected in human blood serum, confirming that it is not only specific to certain cell types but is also released into the bloodstream, enabling less invasive diagnostic procedures. Soon thereafter, it was established that serum PSA levels correlate with the progression of prostate cancer, allowing its use in the diagnosis, staging, and post-treatment monitoring of prostate cancer. Although PSA is also present in healthy individuals, concentrations exceeding 4 ng/ml are generally considered indicative of potential PCa.[1-3]

Despite being one of the most extensively validated biomarkers for making clinical decisions related to prostate cancer, PSA is not currently recommended for general PCa screening. This is due to ongoing debates in the scientific community concerning its limited specificity, as illustrated in Figure 1.

Elevated PSA levels may also result from benign prostatic hyperplasia (BPH), leading to false-positive results, unnecessary biopsies, and undue patient anxiety. This underscores the lack of specificity required for an effective screening tool.

Nevertheless, PSA testing remains a widely used method for tracking disease progression in patients undergoing therapy and is often paired with a digital rectal examination (DRE) for early detection. Regular PSA monitoring is also employed to assess treatment outcomes, including evaluating PSA velocity and doubling time in cancer patients.[4-7]

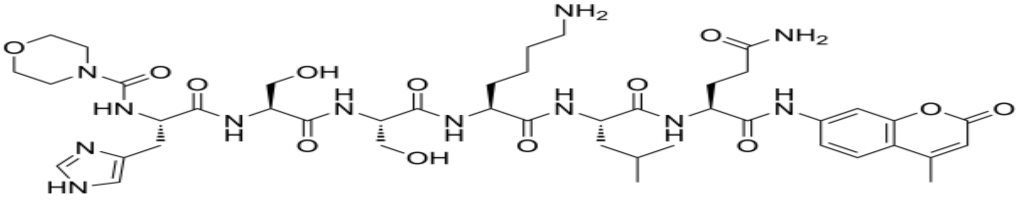

**Figure 1** Chemical structure of PSA

Different methods were used for the determination of FPSA, including biochemical methods [8, 9], analytical methods [10–13], and clinical applications [14, 15].

## 2. Apparatus:

All experiments were conducted using a 797-AV Computrace voltammetric analyzer, a device equipped with an electrode detection system. The working electrode used was a glassy carbon electrode with a diameter of 2 mm, while an Ag/AgCl electrode served as the reference electrode.sat KCl, and 2mm diameter platinum wire as an auxiliary electrode.

A pH meter from Philips was used for pH measurements, and a thermostatic water bath of type haake NK 22 was used to control the temperature.

Volumetric.

## 3. Reagents :

The FPSA pure material was supplied by the French pharmaceutical industry ( biomerieux ). 0.1 g/L of FPSA solution was prepared by diluting 0.1 ml of pure TPSA in 0.9 ml of distilled water.

To prepare the acetate buffer, 41 mL of 0.2 M acetic acid and 9 mL of 0.2 M sodium acetate were combined in a 100 mL volumetric flask, followed by dilution to the final volume using distilled water.

## 4. Procedure :

Differential pulse voltammetry was performed by scanning the potential from -1.0 V to 0.5 V at a scan rate of 0.0125 V/s. Initially, a voltammogram was recorded for 10 mL of acetate buffer (pH 4). Next, the voltammogram for a $1.96 \times 10^{-4}$ M $Mn^{2+}$ solution was obtained, followed by sequential additions of FPSA, with a voltammogram recorded after each addition under the optimized conditions. A calibration curve was constructed based on these sequential additions of FPSA under the optimum conditions. The binding constant was determined at various temperatures (288, 293, 298, 303, and 308 K) using a thermostatic water bath with a voltammetric jacket cell, and the thermodynamic parameters were subsequently calculated.

## 5. Results And Discussion

### 5.1 Indirect estimation of FPSA through its interaction with manganese cation

Indirect estimation of FPSA was carried out through its interaction with manganese cation on a glassy carbon electrode used with an acetate buffer solution at pH 4. By monitoring the decrease in the manganese cation reduction peak current, which appeared at -0.494 V, as a result of FPSA addition.

For this purpose a differential pulse voltammogram of $1.96 \times 10^{-4}$ M manganese cation solution was recorded under the initial default conditions, Table 1, manganese cation shows a well-defined reduction peak at -0.494 V versus Ag/AgCl saturated KCl reference electrode, and Figure 2.

**Table 1**. The initial default conditions for manganese ion reduction

| Parameters | Values |
|---|---|
| S. P. (V) | -1.0 |
| E. P. (V ) | 0 |
| P. A. (V) | 0.05 |
| P. T. (s) | 0.04 |
| V. S. (V) | 0.005 |
| V. S. T. ( s) | 0.4 |
| S. R. ( V/s) | 0.0149 |
| No. C. | 0 |
| C. P. ( V) | -0.1 |
| C. T. (s) | 0 |
| D. P.( V) | -0.9 |
| D. T. (s) | 60 |
| E. T. (s) | 5 |

S.P. : Start potential, E.P. : End potential , P.A. : Pulse amplitude , P. T.: Pulse time , V. S.: Voltage step , V. S. T. : Voltage step time , S.R. : Sweep rate , No. c.: No. of cycles , C.P.: Cleaning potential , C.T.: Cleaning time , D. P. : Deposition potential , D. T. : Deposition time , E. T. : Equilibrium time .

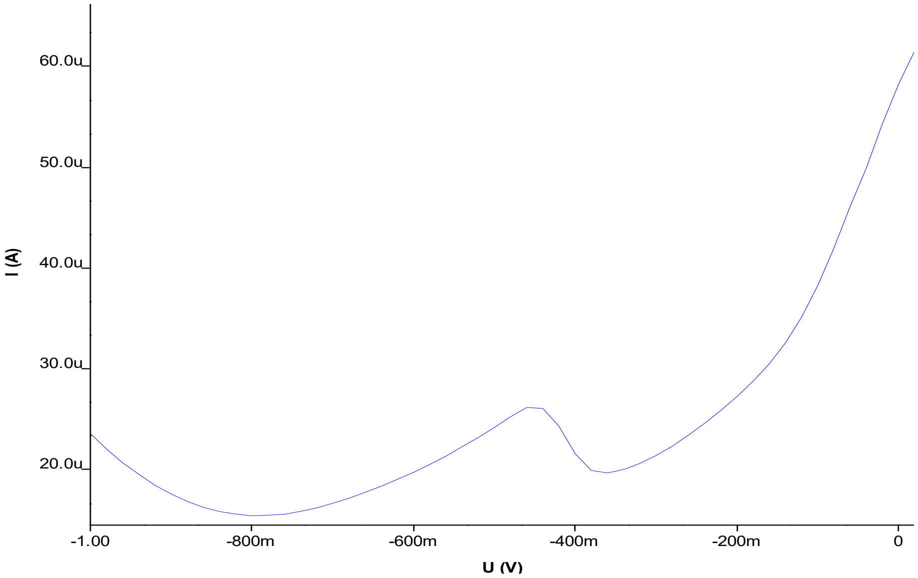

**Figure 2**. The reduction peak of manganese acetate according to the manufacturer's default parameters

### 5.2 Optimum conditions

To examine the optimum measurement conditions, a $1.96 \times 10^{-4}$ M manganese acetate solution was used. Various experimental and instrumental parameters affecting the reduction process of manganese acetate were optimized, including pulse amplitude, pulse time, voltage step, number of cycles, cleaning potential, cleaning time, deposition time, potential, deposition time, and equilibrium time. Table 2 shows the obtained optimum conditions.

**Table 2.** The measured optimum conditions for direct determination of manganese acetate

| Parameters | Values |
|---|---|
| S. P. (V) | -1.0 |
| E. P. (V ) | 0 |
| P. A. (V) | 0.1 |
| P. T. (s) | 0.01 |
| V. S. ( V) | 0.02 |
| No. C. | 4 |
| C. P. (V) | 0.2 |
| C. T. (s) | 3 |
| D. P. ( V) | -0.4 |
| D. T. (s) | 30 |
| E. T. (s) | 1 |

Figure 3: shows the recorded voltammograms for 1.96x10$^{-4}$ M of manganese acetate under the instrument's default conditions (a) and the measured optimal conditions (b), it is evident that the reduction current observed under the optimal conditions was higher than that measured under the default settings of the instrument.

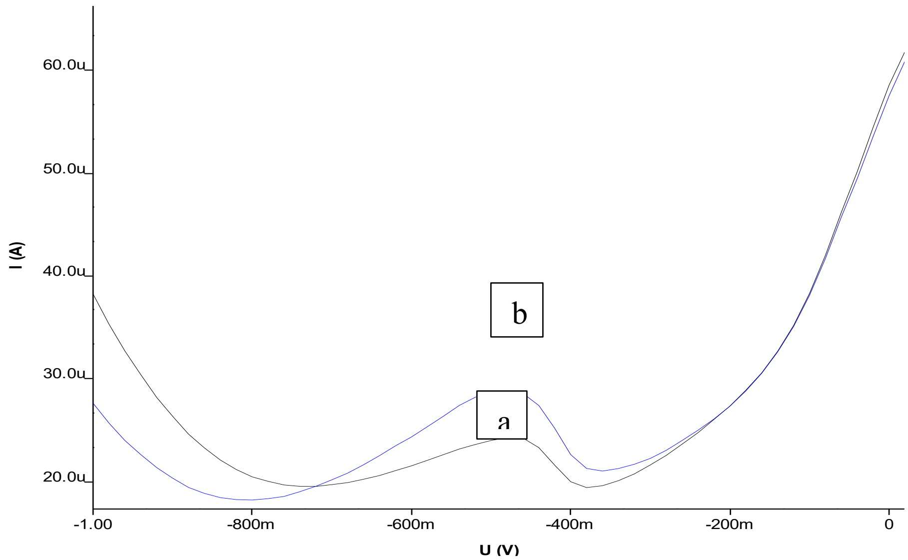

**Figure 3** . Recorded voltammograms of 1.96 × 10⁻⁴ M solution: (a) after and (b) before optimization of the conditions.

**5.3 Stability:**

The stability the of Mn$^{+2}$-FPSA peak was studied by recording the differential pulse voltammogram for various durations period under the optimum measured conditions. The voltammogram was recorded upon addition of 1.38x10$^{-4}$ FPSA to 1.96x10$^{-4}$M Mn$^{+2}$. Solution every five minutes for a total duration time of (50) minutes. It was observed that the current value remained almost constant within the studied time. The results are shown in Table 3.

**Table 3.** Shows the stability of the reduction peak current

| Time (min.) | Ep(V) | Ip µ A |
|---|---|---|
| 0 | -0.46 | 17.2 |
| 5 | -0.46 | 17.0 |
| 10 | -0.46 | 18.3 |
| 15 | -0.46 | 19.0 |
| 20 | -0.46 | 19.5 |
| 25 | -0.46 | 20.6 |
| 30 | -0.46 | 21.2 |
| 35 | -0.46 | 21.9 |
| 40 | -0.46 | 22.2 |
| 45 | -0.46 | 22.6 |
| 50 | -0.46 | 22.9 |

### 5.4 Effect of pH :

It is noted that there is a decrease in the diffusion current with an increase in the supporting medium electrolyte acidity, except at pH4, which indicates a significant increase in the current value and provides the best reduction wave shape. Therefore, it was chosen as an ideal pH for studying the electrochemical behavior of FPSA in the presence of the manganese ion Table(4).

**Table 4.** Shows the pH of the reduction peak current

| pH | Ep (V) | ΔIp µA |
|---|---|---|
| 2 | -0.48 | 1.61 |
| 3 | -0.50 | 0.90 |
| 4 | -0.49 | 4.40 |
| 5 | -0.50 | 0.88 |
| 6 | -0.50 | 0.32 |

### 5.5 Calibration curve:

A calibration curve was generated by adding the sequence of standard solutions additions of a $6.89 \times 10^{-6}$M FPSA in the presence of 500 µL of $10^{-2}$ M manganese ion in acetate buffer solution (pH4). The voltammogram was measured under the measured optimum conditions for each addition of FPSA, Figure 4.

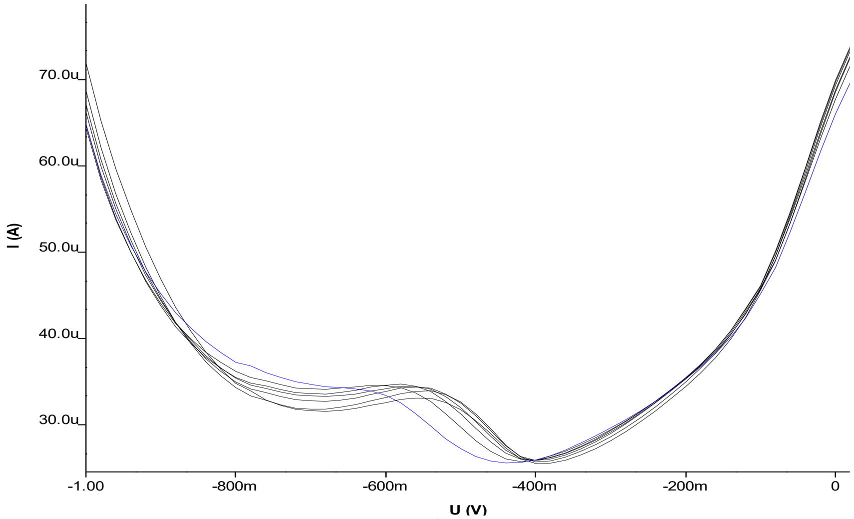

**Figure 4.** Differential pulse voltammograms of ($4.76 \times 10^{-4}$) M manganese ion in the presence of a range of amounts of FPSA.

The graph of reduction peak current against concentration yields a straight line, Figure 5 . in the concentration range (5.498 – 13.663) x$10^{-7}$ M with a calibration equation y = 0.0073x+0.6451 and correlation coefficient equal to 0.9581.

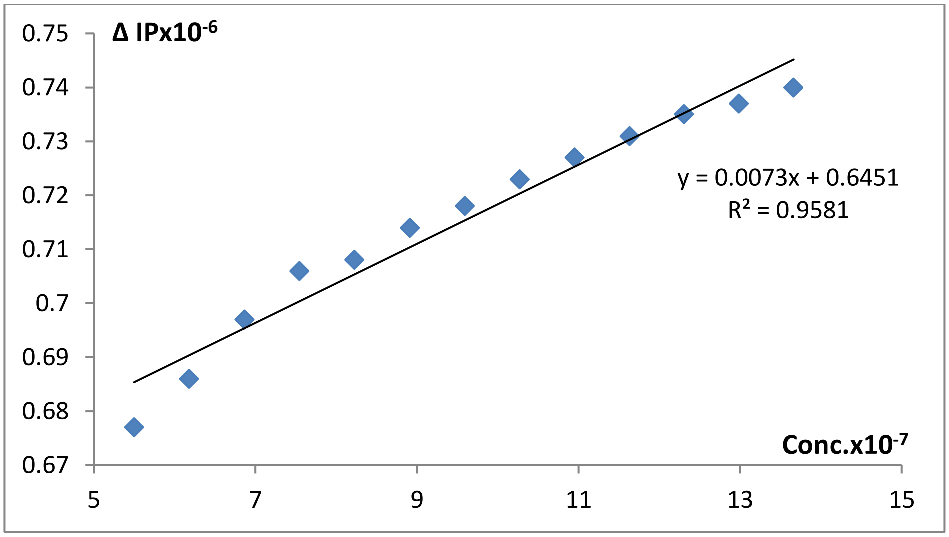

**Figure 5 .** Calibration curve of FPSA under the measured optimum conditions.

### 5.6 Thermodynamic Calculations

The binding constant for the interaction between FPSA and manganese ions was determined using the following equation (1):

$$\ln (Ip/(Ip°-Ip)) = \ln (1/[Conc.]) - \ln K_b \qquad .....(1)$$

In this equation, Ip° represents the reduction current of manganese ions alone, Ip denotes the reduction current of the FPSA–manganese complex, [Conc.] refers to the molar concentration of manganese ions ($10^{-2}$ M), and Kb is the binding constant for the FPSA–manganese complex. The binding constant was determined at various temperatures (288, 293, 298, 303, and 308 K), and the corresponding results are presented in Table 5.

Table 5.. The binding constant of FPSA – manganese complex at different temperatures

| Temp (K) | 1/ T $K^{-1}$ | Ln $K_b$ |
|---|---|---|
| 288 | 0.0034722 | 27.519 |
| 293 | 0.00341296 | 21.633 |
| 298 | 0.00335570 | 19.705 |
| 303 | 0.00330033 | 18.251 |
| 308 | 0.00324675 | 16.119 |

Thermodynamic parameters were calculated using Van't Hoff equation (equation 2)

$$\mathrm{LnK} = -\frac{\Delta H}{RT} + \frac{\Delta S}{R} \qquad .......(2)$$

Enthalpy (ΔH) was determined from the slope Van't Hoff equation

$$\Delta H = - \text{Slope} \times R \qquad ......(3)$$

(R= 8.314 J. $mole^{-1}$ . $K^{-1}$)

The free energy (ΔG) was determined from (equation 4 )

$$\Delta G = - R \times T \times \ln K_b \qquad ......(4)$$

Entropy (ΔS) was determined from the intercept of the Van't Hoff equation (equation 5)

$$\Delta S = \text{Intercept} \times R \qquad .....(5)$$

The plot of ln K versus 1/ T results in a straight-line plot with $R^2$ equal to 0.9191, Figure 6.

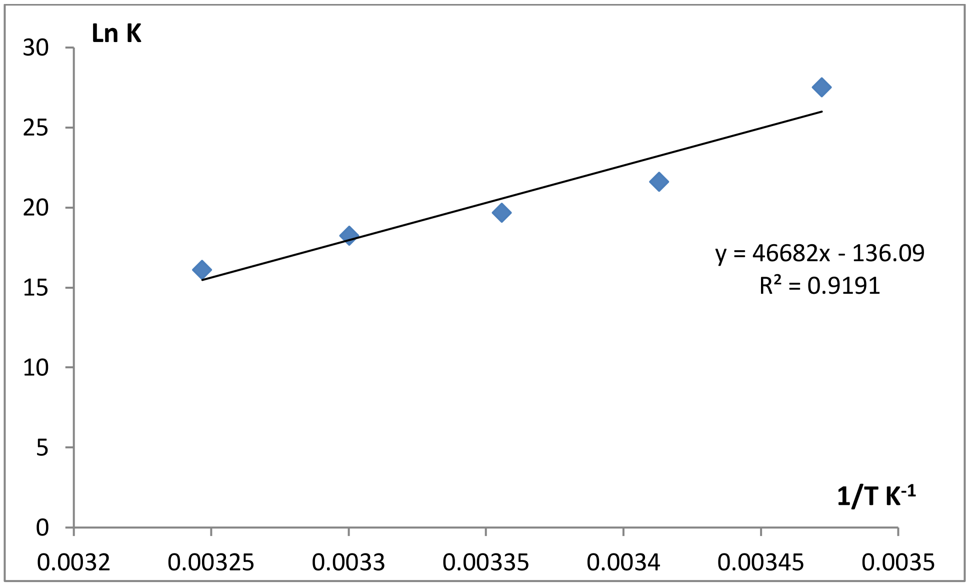

**Figure 6.** Relation between ln k and 1/ T

Thermodynamic values for FPSA– manganese interaction were tabulated in Table 6

**Table 6.** Thermodynamic values for FPSA – manganese interaction

| Temp(K) | ΔH(KJ/mol) | ΔG(KJ/mol) | ΔS(J/mol.K) |
|---|---|---|---|
| 288 | -388.114 | -65.892 | -1131.452 |
| 293 | | -52.698 | |
| 298 | | -48.820 | |
| 303 | | -45.976 | |
| 308 | | -41.276 | |

The negative value of ΔH suggests that the interaction between FPSA and manganese ions is exothermic. Consequently, the binding constant decreases with increasing temperature this lies in agreement with the negative value of ΔH. Additionally, the increase in ΔG with temperature indicates a reduction in the spontaneity of the binding process as temperature rises, this also indicates why the value of the binding constant decreases as the temperature increases. The negative value of ΔS implies that the system becomes more ordered upon complex formation. Together, the negative ΔH and ΔS values indicate that the interaction is both enthalpy and entropy driven, likely involving the formation of coordination bonds between manganese ions and FPSA.[16-25.]

## 6. Conclusion

The electrochemical behaviour of FPSA can be done indirectly, in acetate buffer solution pH4, by following the decrease in manganese reduction peak current which appeared at -0.494 V as a result of FPSA added. The binding constant was calculated and thermodynamic values were examined. The results of the thermodynamic study indicates that the binding is primarily driven by both enthalpic and entropic contributions, and the interaction may involve the formation of a coordination interaction bond between manganese and FPSA.

## 7. Acknowledgements

The authors wish to thank the University of Mosul /College of Science/ Department of Chemistry for allowing us to use their facilities

## 8. References

[1] F. Islami, K. Miller, R. Siegel, Z. Zheng, J. Zhao, X. Han, and K. Yabroff. National and state estimates of lost earnings from cancer deaths in the United States. JAMA oncology, no.5(9), e191460-e191460,2019. doi:10.1001/jamaoncol.2019.1460.

[2] I. V. Maly, and W. A. Hofmann. Calcium and nuclear signaling in prostat cancer. International journal of molecular sciences, no.19(4), 1237, 2018. https://doi.org/10.3390/ijms19041237.

[3] V. K. Sarhadi, and G. Armengol. Molecular biomarkers in cancer. *Biomolecules*, *12*(8), 1021,2022. https://doi.org/10.3390/biom12081021.

[4] M. Mascini and S. Tombelli, Biosensors for biomarkers in medical diagnostics,Biomarkers .no.13 , 637-657, 2008. https://doi.org/10.1080/13547500802645905.

[5] D.A. Healy, C.J. Hayes, P. Leonard, L. McKenna and R. O'Kennedy, Biosensor developments: application to prostate-specific antigen detection, TRENDS Biotech. no. 25 , 125-131 ,2007. doi: 10.1016/j.tibtech.2007.01.004 .

[6] S. Liu, X. Zhang, Y. Wu, Y. Tu, L. He, Prostate-specific antigen detection by using a reusable amperometric immunosensor based on reversible binding and leasing of HRP-anti-PSA from phenylboronic acid modified electrode, Clin. ,Chim Acta . no. 395 , 51-56 , 2008. https://doi.org/10.1016/j.cca.2008.04.031.

[7] Y. Zheng, Y. Yuan, Y. Chai, and R. Yuan, A label-free electrochemical aptasensor based on the catalysis of manganese porphyrins for detection of thrombin, Biosens. Bioelectron. no.66 , 585-589, 2015. https://doi.org/10.1016/j.bios.2014.12.022.

[8] P. Damborský, D. Damborská, Š. Belický, J. Tkáč, , and J. Katrlík,. Sweet strategies in prostate cancer biomarker research: Focus on a prostate specific antigen. BioNanoScience. no.8, 690-700 , 2018. https://doi.org/10.1007/s12668-017-0397-z .

[9] S. P. Balk, Y. J. Ko, , and G. J. Bubley,. Biology of prostate-specific antigen. Journal of clinical oncology. no.21 (2) , 383-391, 2003. https://doi.org/10.1200/JCO.2003.02.083.

[10] D. Damborska , T. Bertok , E. Dosekova, A. Holazova,L. Lorencova ,P. Kasak, and J. Tkac.. Nanomaterial-based biosensors for detection of prostate specific antigen. Microchimica acta . no. 184, 3049-3067, 2017. https://doi.org/10.1007/s00604-017-2410-1.

[11] T. Vermassen, M. Speeckaert , N. Lumen, S. Rottey, and J. R. Delanghe. Glycosylation of prostate specific antigen and its potential diagnostic applications. Clinica chimica acta, no.413, 1500-1505, 2012. https://doi.org/10.1016/j.cca.2012.06.007.

[12] A. Thakur, A. Kumar. Exploring the potential of ionic liquid-based electrochemical biosensors for real-time biomolecule monitoring in pharmaceutical applications: from lab to life. Results in Engineering. no.20 , 101533 , 2023. https://doi.org/10.1016/j.rineng.2023.101533.

[13] V. Vanova , K. Mitrevska , V. Milosavljevic ,D. Hynek , L. Richtera , and V. Adam. Peptide-based electrochemical biosensors utilized for protein detection. Biosensors and Bioelectronics, no.180, 113087, 2021. https://doi.org/10.1016/j.bios.2021.113087.

[14] K. Duskova , and S. Vesely . Prostate specific antigen. Current clinical application and future prospects. Biomedical Papers of the Medical Faculty of Palacky University in Olomouc.no.1, 159, 2015. http://dx.doi.org/10.5507/bp.2014.046.

[15] J. H. Hayes , and M. J. Barry. Screening for prostate cancer with the prostate-specific antigen test: a review of current evidence. Jama. no. 311(11) , 1143-1149 , 2014. doi:10.1001/jama.2014.2085.

[16] A. Th. AL-Taee, and A. Z. AL-Hafidh, Research Journal of Pharmacy and Technology,14, 6541, 2021. http://dx.doi.org/10.52711/0974-360X.2021.01131 .

[17] A. M. AL-hasany, A. Th. AL-Taee, and H. A. AL-wahb, The Eurasia Proceedings of Science Technology Engineering and Mathematics. 7, 204 , 2019. ISSN: 2602-3199 .

[18] M. Q. Hasan , A. Th. Al-Taee , and M. M. Al-Imam. Electrochemical Behavior of Finasteride on Glassy Carbon Electrode Using Differential Pulse Voltammetric Technique. Analytical and Bioanalytical Electrochemistry. 16(8) ,752-763, 2024. https://www.doi.org/10.22034/abec.2024.715425.

[19] M. A. Al-Imam and F. M. Al-Abady, Electrochemical behavior of aspartic amino acid and its molecular interaction with Mn (II) ions at different conditions using SWV method. 1, 2394, 2022. https://doi.org/10.1063/5.0121576 .

[20] A. R. Jalalvand, "Fabrication of a novel and ultrasensitive label-free electrochemical aptasensor for detection of biomarker prostate specific antigen." International journal of biological macromolecules 126 , 1065-1073, 2019 . https://doi.org/10.1016/j.ijbiomac.2019.01.012

[21] F. E. Martinez-Rojas, , and A. Francisco, "Conducting polymer applied in a label-free electrochemical immunosensor for the detection prostate-specific antigen using its redox response as an analytical signal." Journal of Electroanalytical Chemistry 880 , 114877, 2021. https://doi.org/10.1016/j.jelechem.2020.114877

[22] L. Han, D. Wang, L. Yan, V. A. Petrenko, and A. Liu, Specific phages-based electrochemical impedimetric immunosensors for label-free and ultrasensitive detection of dual prostate-specific antigens. Sensors and Actuators B: Chemical, 297, 126727, 2019. https://doi.org/10.1016/j.snb.2019.126727

[23] S. M., Traynor, R. Pandey, R. Maclachlan, A. Hosseini, T. F.Didar, F. Li, and L. Soleymani, recent advances in electrochemical detection of prostate specific antigen (PSA) in clinically-relevant samples. Journal of The Electrochemical Society, 167(3), 037551., 2020. **Doi:**10.1149/1945-7111/ab69fd.

[24] F. S., Tabar, M., Pourmadadi, H. Rashedi, and F. Yazdian, Design of electrochemical nanobiosensor in the diagnosis of prostate specific antigen (PSA) using nanostructures. In 2020 27th National and 5th International Iranian Conference on Biomedical Engineering (ICBME) (pp. 35-40). 2020. **DOI:** 10.1109/ICBME51989.2020.9319418

[25] C. Thunkhamrak, P. Chuntib, K. Ounnunkad, P. Banet, P. H. Aubert, G. Saianand, and J. Jakmunee, Highly sensitive voltammetric immunosensor for the detection of prostate specific antigen based on silver nanoprobe assisted graphene oxide modified screen printed carbon electrode. Talanta, 208, 120389, 2020 . https://doi.org/10.1016/j.talanta.2019.120389

# التقدير الغير المباشر للمستضد البروستاتي النوعي الحر على قطب الكاربون الزجاجي من خلال التداخل مع خلات المنغنيز باستخدام تقنية الفولتامتري النبضي التفاضلي

**محمد قحطان حسن (1)، عامر ذنون الطائي (2)، محمد محمد أمين الأمام (3)**

(1,2) قسم الكيمياء ,كلية العلوم ، جامعة الموصل ، الموصل ، العراق
(3) قسم الكيمياء، كلية التربية للعلوم الصرفة ، جامعة الموصل ، الموصل ، العراق

**الخلاصة:**

تمت دراسة السلوك الكهروكيميائي غير المباشر للمستضد البروستاتي النوعي الحر FPSA باستخدام تقنية الفولتامتري النبضي التفاضلي، و بنظام ثلاثي الأقطاب يتكون من قطب عامل من الكربون الزجاجي بقطر 2 مم، وقطب مساعد يتكون من سلك بلاتين بقطر 2 مم، وقطب مرجع من الفضة/كلوريد الفضة المشبع بكلوريد البوتاسيوم (Ag/AgCl sat KCl) . تستند الطريقة إلى مراقبة الانخفاض في تيار ذروة اختزال ايون المنغنيز، والذي يُعزى إلى تفاعله مع مركب FPSA و باستخدام محلول الخلات المنظم (pH=4) ، وتم مسح الجهد بين -1.0 فولت إلى 0.5 فولت، كما تم اختبار الظروف المثلى للقياس.

تم انشاء المنحني القياسي للـFPSA باستخدام الاضافات المتتابعة ، وكان الخط مستقيماً ضمن مدى التركيز المدروس (5.498 - 13.663) × $10^{-7}$ مولاري ، بمعامل ارتباط بلغ 0.9581، ومعادلة الخط المستقيم $y = 0.0073x + 0.6451$ كما تم حساب ثابت الارتباط (k) والقيم الثرموديناميكية ($\Delta G$ ، $\Delta H$، $\Delta S$) لتفاعل $Mn^{2+}$ - FPSA .